ORIGINAL ARTICLE

lajss.org© Latin American Journal of Solids and Structures

www.lajss.org

Analysis of the effect of localized corrosion shape on a cracked and notched 2024 AL plate repaired with composite patch under thermo-mechanical loading

Hayet Benzineb[a], Mohamed Berrahou[a*], Leila Belkaddour[a]

[a] Laboratory of Industrial Engineering & Sustainable Development – GIDD, Faculty of Technology, Université de Relizane, CitéBourmadia, W. Relizane, 48000, Algeria. E-mail: amarikaoula539@gmail.com, berrahou22@yahoo.com, lailabelkadour@gmail.com

* Corresponding author.

https://doi.org/10.1590/1679-78257415

Abstract

This study highlights the analysis of corrosion shape effects under thermo-mechanical loading on the development of damage in corroded and cracked aluminum plates. This study is divided into two parts, the numerical analytical part, was performed to compare the effect of the corrosion geometry on the repair and adhesive damage; We analyzed the effects of damaged areas on the level of corrosion in the adhesive layer of three composite materials (boron/epoxy, glass/epoxy, and graphite/epoxy), and studied the change of the stress intensity factor for circle or square-shaped corrosion. The second part related to an experimental study of the corrosion shape on the ultimate strength of the damaged plate repaired by the boron/epoxy composite material. The results obtained, indicated that the effect of the circular shape of corrosion is small compared to the square shape. The type of composite material (boron / epoxy) has proven its optimal effect on repair.

Keywords

Composite repair, Corrosion, Crack, Stress intensity factor (SIF), Thermo mechanical Loadings, Damaged area ratio (D_R), Ultimate strength σ_u.

Graphical Abstract

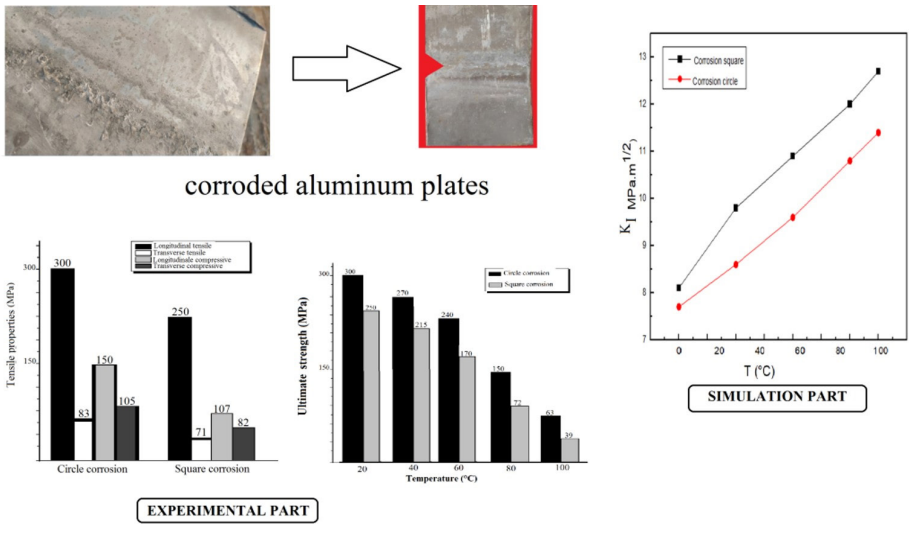

Received: December 17, 2022. In revised form: December 29, 2022. Accepted: January 23, 2023. Available online: January 24, 2023.
https://doi.org/10.1590/1679-78257415

1 INTRODUCTION

In order to study, optimize and extend the life of bonded assemblies, a variety of experimental and analysis models have been developed studying the aspects of formulation, implementation, characterization and aging or durability of adhesives and bonded assemblies. Several researchers studied cracks in the structure (Liu et al. 2019; Blond and Mouro 1999; Bouchekara et al. 2021), corrosion(Karatzas et al. 2013; Ely et al. 2017;Chegeni et al.2019), or both at the same time (Nakano et al. 2012; Umamahshwer Rao et al. 2016; Wei et al. 2021) with or without repairs.

In aluminum alloys, localized corrosion is a common occurrence due to surface defects at the passive film level. This subject has been extensively investigated in the literature. According to researches, localized corrosion on metals can occur rapidly because of fatigue or stress, causing structural damage. Studies have been conducted on localized corrosion on aluminum, such as the susceptibility to intergranular corrosion of the 2024 Al alloy during re-aging after solution treatment and cold rolling (Wang et al. 2016). A high-resolution 2D and 3D electron imaging study of the de-alloying of the S phase (Al2CuMg) in the aluminum alloy AA 2024-T3 was conducted by(Hashimoto et al. 2016).

During mechanical loading of materials with elasto-plastic behavior, the crack tip blunts and propagates based on the stress distribution. In order to evaluate the change in the concentration of stresses in the damaged zone, SIF in the vicinity of the crack must be studied. In order to offer the best repair model, several models have been developed, studying the stress field in the adhesive layer and composite(Benyahia et al. 2014), optimizing the shape of composite patch (Ramji et al. 2013), analyzing the rupture of substrate/patch bonding adhesives (Berrahou and Bouiadjra 2016), and the optimization of the repair of a cracked plate by composite patches treated by microwaves (Xiaoyau et al. 2019). These studies have led to close and distinct results, according to chosen parameters for the repaired structure.

Damaged zone theory has been studied in recent literature; these studies have analyzed adhesive damage (Albedah et al. 2011; Chang–Su, et al. 2008), optimal patch shapes (Bouanani et al. 2013), and shear stresses, which has an important part in the damage of adhesives (Shishesaz and Reza2013).

In this work, experimental tests had been made on rectangular aluminum 2024 T3 corroded and cracked plate with different shapes of localized corrosion (circular and square shapes).Similarly, we simulate and evaluate the effects of corrosion geometrical shapes on the stress's evolution of welded assemblies, using an AL 2024 T3 plate with V-notch cracked and corroded, repaired by different types of composite patches under thermo-mechanical loading. To evaluate the results of experimental and the simulation works, we have examined the effects of corrosion geometry on the stresses around the crack and corrosion, analyzing crack length variations and thermal variations on SIF and investigating variations on adhesives layer as well.

2 RESULTS AND ANALYSIS

This research consists of two parts. The first part relates to the use of the Finite Element Method (FEM) to find out the types of composite materials and the appropriate shapes for corrosion repair, whether corrosion in the shape of a circle or a square shape under thermo-mechanical loading. After making sure in the analytical part of the appropriate type for repairing corroded structures, in the second part, an investigation is made to select which shapes of corrosion affect structures the most. We carried out experimental research on corrosion-prone aluminum plates (i.e., corrosion in the form of a circle or square) and treated them with boron/epoxy composite materials, where fiber orientations are directed in tensile strength direction (longitudinal direction Θ= 0°).

2.1 simulation part

This study is carried out on AL 2024-T3 plate with V-notch with an angle α=60°.The dimensions of the plate are the length H_{pl}= 204 mm, the width W_{pl}= 152mm with thickness e_{pl}= 2mm. It is assumed that the crack emanating from the notch is straight and has different depths.

In Figure 1, the plate is stressed under uniaxial tensile in the longitudinal direction "y" of 150MPa of stress and embedded in opposite side.

The corrosion geometric shape examined are square and circle form with a thickness 0.25 mm. Before repairing the structure, the corroded area is cleaned to remove the Corrosion film and keep the same mechanical properties. We will analyze this shape in two regular shapes: circular with radius R=30mm and square with dimension L =30mm, the patch thicknesses e_{pat} = 1.5mm glued with FM73 adhesive with a thickness e_{ad} =0.127mm.All mechanical and thermal properties materials are shown in Table 1; Obtained from Salem et al. (2017).

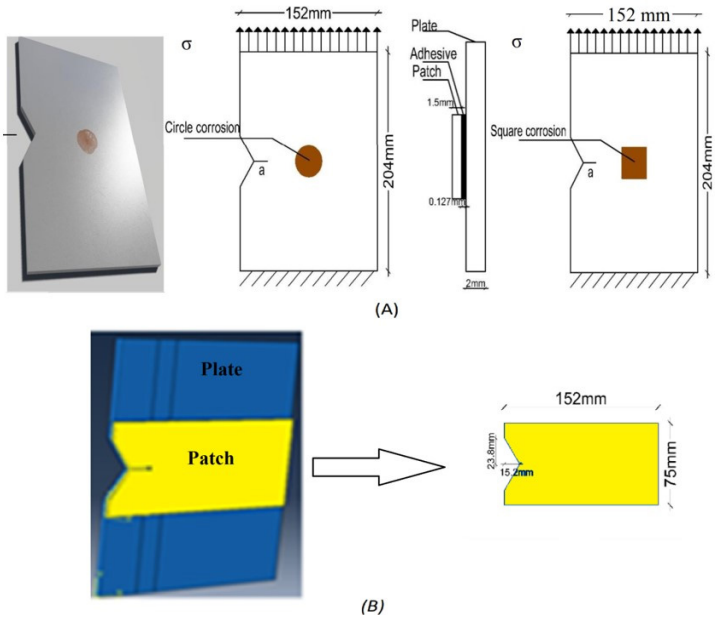

Figure 1 Geometric model: (A) of the AL plate with corrosion and (B) the shape of patch.

Table 1 Mechanical and thermal properties of all materials

	Al 2024	FM-73	Boron/Epoxy	Glass/Epoxy	Graphite/Epoxy
E_1 (GPa)	72		200	50	127.5
E_2 (GPa)			19.6	25	9.00
E_3 (GPa)			19.6	25	4.80
υ_{12}	0.3	0.32	0.3	0.21	0.342
υ_{13}			0.28	0.21	0.342
υ_{23}			0.28	0.21	0.38
G_{12} (GPa)		4.2	7.2	7.2	4.8
G_{13} (GPa)			5.5	5.5	4.8
G_{23} (GPa)			5.5	5.5	2.55
$\alpha_{12}(10^{-6}\ C°)$			4.5	5.5	-1.2
$\alpha_{13}(10^{-6}\ C°)$			23	15	34
$\alpha_{23}(10^{-6}\ C°)$			23	15	34

The three-dimensional finite element method is used to analyze the model of this study using the ABAQUS software (Abaqus 2007). The finite elementmesh was generated using brick elements with 20 nodes. The FEM model simulates the plate, the adhesive and the composite patch. The number of elements used in this study: is 37062 elements for the aluminum plate, 17024 elements for the glue layer and 17024 elements for the composite patch. Figure 2 presents the FEM mesh of the plate and around the point of the crack; the mesh is refined in the crack front to have better results.The total number of elements of the structure is 71000 quadratic hexahedral elements of type C3D20R, with 68829 nodes. The geometric shape of the crack is 3d. The plate has eight layers of elements in the thickness direction, the adhesive has only one layer of elements through thickness and the patch has four layers of elements through thickness. To generate crack front some brick elements are replaced by “crack block”. These crack-blocks are meshes of brick elements which are mapped into the original element space and merged with surrounding mesh.

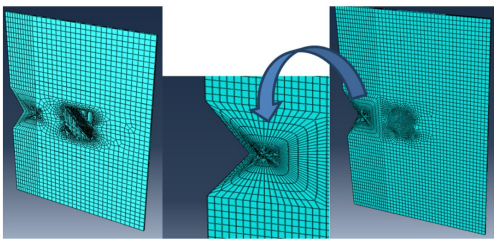

Figure 2 Plate mesh.

2.1.1 Effect of crack length on Variations of SIF (K_I) as a function of temperature variation (ΔT)

The stress intensity factor "K" is the main parameter for the evaluation of the integrity of structures containing cracks, which must be calculated with great precision in order to evaluate the evolution of the crack under stress. The 3D FEM method is used to determine the stress and strain field as well as the stresses at the crack tip.

The Von-Mises criterion is introduced to model the material non-linearity of the adhesive. The stress intensity factors at the crack tip are calculated using the virtual crack technique. They are obtained for the 03 modes by the following equation (eq.1):

$$\mathbf{G_i = Ki^2 / E} \tag{1}$$

G: the energy release, Ki: is the SIF; E: is the Young's modulus.

The model referred to above is called the linear elastic fracture mechanics model and has found wide acceptance as a method for determining the resistance of a material to below-yield strength fractures. The model is based on the use of linear elastic stress analysis; therefore, in using the model one implicitly assumes that at the initiation of fracture any localized plastic deformation is small and considered within the surrounding elastic stress field.

$$\boldsymbol{\sigma_x = \frac{K}{\sqrt{2\pi r}}\cos\frac{\theta}{2}\left[1-\sin\frac{\theta}{2}\sin\frac{3\theta}{2}\right]}$$

$$\boldsymbol{\sigma_y = \frac{K}{\sqrt{2\pi r}}\cos\frac{\theta}{2}\left[1+\sin\frac{\theta}{2}\sin\frac{3\theta}{2}\right]} \tag{2}$$

$$\boldsymbol{\sigma_{xy} = \frac{K}{\sqrt{2\pi r}}\sin\frac{\theta}{2}\left[\cos\frac{\theta}{2}\cos\frac{3\theta}{2}\right]}$$

The stress in the third direction are given by $\sigma_z = \sigma_{xz} = \sigma_{yz} = 0$ for the plane stress problem, and when the third directional strains are zero (plane strain problem), the out of plane stresses become $\sigma_{xz} = \sigma_{yz} = 0$ and$\sigma_z = \vartheta(\sigma_x + \sigma_y)$. While the geometry and loading of a component may change, as long as the crack opens in a direction normal to the crack path, the crack tip stresses are found to be as given by Equations 6.

The stress intensity factor (K) is used in fracture mechanics to predict the stress state "stress intensity" near the tip of a crack or notch caused by a remote load or residual stresses. It is a theoretical construct usually applied to a homogeneous, linear elastic material and is useful for providing a failure criterion for brittle materials, and is a critical technique in the discipline of damage tolerance. The concept can also be applied to materials that exhibit small-scale yielding at a crack tip.

The magnitude of K depends on specimen geometry, the size and location of the crack or notch, and the magnitude and the distribution of loads on the material. It can be written as (Soboyejo 2003; Janssen 2004):

$$\mathbf{K = \sigma\sqrt{\pi a} f\left(\frac{a}{W}\right)} \tag{3}$$

Where: $\mathrm{f}(\frac{\mathrm{a}}{\mathrm{W}})$ is a specimen geometry dependent function of the crack length a, the specimen width W, and σ is the applied stress.

In 1957, G. Irwin found that the stresses around a crack could be expressed in terms of a scaling factor called the stress intensity factor. He found that a crack subjected to any arbitrary loading could be resolved into three types of linearly independent cracking modes (Suresh 2004).These load types are categorized as Mode I. Mode I is an opening (tensile) mode where the crack surfaces move directly apart.

The stress intensity factor for mode I is designated K_I and applied to the crack opening mode. This factor is formally defined as (Rooke and Cartwright 1976):

$$\boldsymbol{K_I = \lim_{r\to 0}\sqrt{2\pi r}\,\sigma_{yy}(r,0)} \tag{4}$$

$$\boldsymbol{K_I = \alpha\beta\sqrt{\pi a}} \tag{5}$$

With:

$$\boldsymbol{\beta = (1 - 0.025\alpha^2 + 0.06\alpha^4)\sqrt{sec\frac{\alpha\pi}{2}}}$$

Where,
K_I=Stress intensity factor
β = Geometry factor
α = 2a/W
2a = Crack length
W = Width of the plate
σ = Force applied
Where the factor β is used to relate gross geometrical features to the stress intensity factor

$$\boldsymbol{K_I = \sigma\sqrt{\pi a}\left[\frac{1-\frac{a}{2b}+0.326(\frac{a}{b})^2}{\sqrt{1-\frac{a}{b}}}\right]} \quad (6)$$

Figure 3 presents the variations of SIF as a function of temperature variations (ΔT) under uniaxial tensile mechanical stresses of σ = 150Mpa, using normal patch shape for the repair.

The behavior of the graphs is almost similar and they are increasing with the increase of temperature. For the effect of square shape of corrosion model, we note that at the interval T=[0°C, 30°C], the stresses are minimal and increasing rapidly with temperature variations T, but when the temperature increases and exceeds 30°C, the stresses increases slightly. However, for the circular shape of corrosion model, the graphs are increasing with the same rate of temperature (T) increases. We note that SIF values are minimal for the model with circular shape of localized corrosion than the other one by up to 30%. As for the comparison between the composites types, the SIF values of graphite/epoxy are the highest, and this type is more sensitive to temperature changes than the others types. The optimal type was boron/epoxy since it had the lowest SIF values.

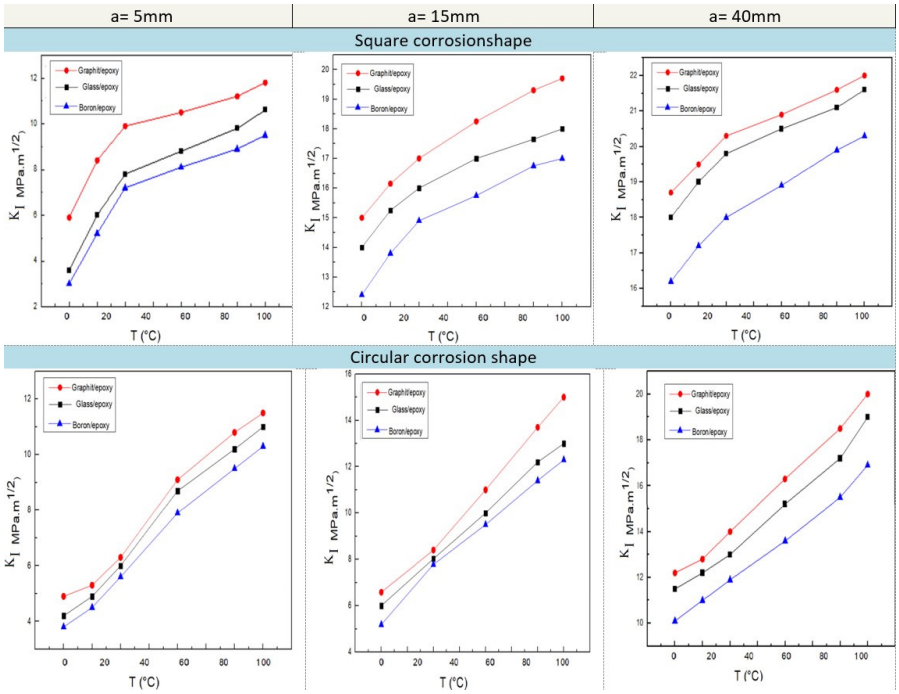

Figure 3 Variation de SIF en fonction de la température (ΔT) for different crack length.

2.1.2 Effect of corrosion shape on Variations of SIF (K_I) as a function of temperature variation (ΔT)

This study was made for a crack length a = 40 mm under tensile stress σ= 150MPa and temperature variations (ΔT), using only boron/epoxy type patch, because in the previous paragraph, it proved to be the best type compared to the

other types in this study.Figure 4 shows that the graphs are ascending and they increase with the increase of temperature, the values of stress intensity factors IF in case of circular shape corrosion model are minimal compared to those of square shape of corrosion model. This illustrates that the circular geometric shape of corrosion influences the stress state of the bonded assembly less than the square-shaped corrosion. This may explain that de geometric of square corrosion is more influencing for its square borders which is not letting the flow of stresses move easily, and that increase the constraints in those borders.

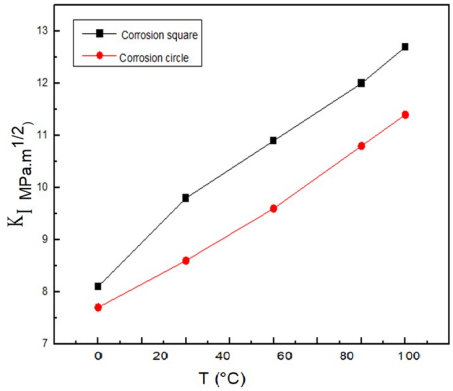

Figure 4 Variation of SIF as a function of temperature (ΔT) for different corrosion shapes.

2.1.3 Von Mises variations as a function of normalized horizontal path distance

This study was made for a crack length a = 15 mm, under temperature T= 60°C for the two models which have the two shapes of circular and square shape of corrosion; using only boron/epoxy type for the repair.

The path is measured according to crack length of the horizontal path. We note at figure 5 that the Von-Mises stress values starts with a high value at the notch tip, whenσ_{xx}= 300MPa for the model that contains the circular corrosion shape, and σ_{xx}=500MPa for the second model. The Von Mises values increases suddenly at the crack tip to reach σ_{xx}=750MPa for the first model (circular corrosion) and σ_{xx}=1260MPa for the second one (square corrosion). After that, the graphs descend fast beyond the crack front; these stresses are low at the corrosion level, which illustrates that the Von stresses variations at corrosion level are minimal comparing to the stress variations at the crack front, almost negligible. Then, these stresses run down to σ_{xx}=85MPa at the plate edge for circular corrosion andσ_{xx}=240MPa for square corrosion.

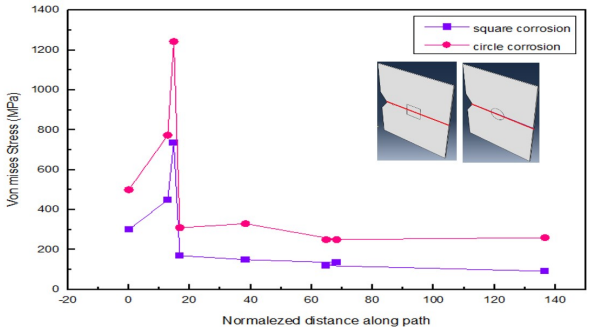

Figure 5 Variation of Von-Mises stress σ_{xx} as function of a normalized distance along horizontal path.

2.1.4 Variations of the Von Mises stresses as a function of the normalized path distance (vertical path)

Figure 6 shows the variations of the Von-Mises stresses as a function of the normalized distance of the vertical path passing through the crack front under the same conditions as the horizontal path.

The graphs are similar and have the same inclination. We note that the graphs begin with a slight rise in Von-Mises stresses on the upper and lower edge points of the plate, where the tensile stresses are applied on one side as well as the embedding in the other side, under thermal loads. Then these stresses decrease slightly but at the crack front increases fast to a maximum point, whenσ_{yy}=875MPa for the model which have the circular corrosion shape and σ_{yy}=1230MPa for the second one.

It is noted that the Von-Mises stresses in case of a circular corrosion shape model are always minimal compared to those of the square corrosion shape model.

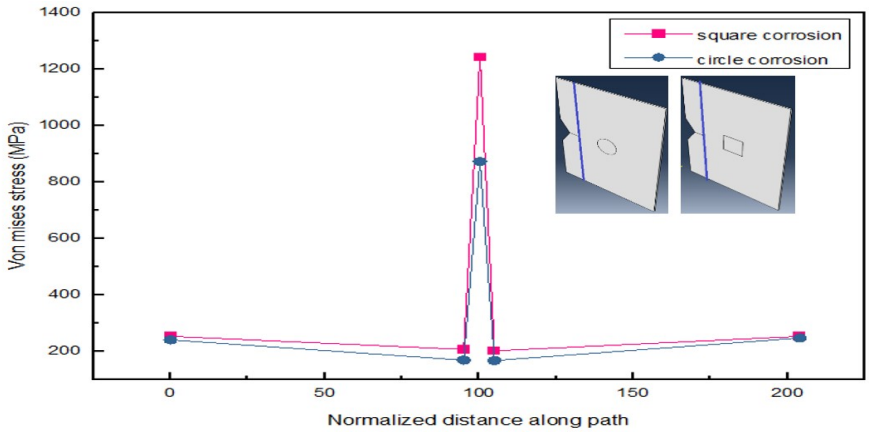

Figure 6 Variation of Von-Mises stress σ_{yy}as function of a normalized distance along vertical path.

2.1.5 Analysis of damaged area ratio (D_R)

This study was made to determine the evolution of damaged area in adhesive joint in bonded assemblies. The damaged zone criterion was proposed by (Sheppard et al. 1998) for the analysis of adhesive joints damage in bonded assemblies. (Chang-Su et al. 2008)introduced modifications to the above-cited damaged area model; the damaged area ratio was suggested to predict the failure load of adhesive joint.

For the FM73 adhesive, the ratio of damaged area D_R has been shown to be approximately 0.2474 [22].The damaged area ratio D_R is defined as follows:

$$\mathbf{D_R = \sum Ai \,/\, L \,.W} \tag{7}$$

Ai: the surface on which the equivalent strain exceeds 7.87%.

L: adhesive length. W: adhesive width.

The plate is subjected to a uniaxial tension of σ=150MPa and temperature variations (ΔT) from (T=0°C) to (T=100°C).This theory is used to analyze the thermo-mechanical effect on adhesive damage in bonded assemblies in AL 2024 T3 plates repaired by composite patches of several types.

2.1.5.1 Analysis of FM73 adhesive damage:

Since the effect of corrosion is negligible compared to the effects of the crack in terms of stresses, the study of D_R was made for the two models(square and circular corrosion shape) and for different patch type (boron/epoxy, glass/epoxy and graphite/epoxy).This study was carried out with the aim to illustrate the evolution of damaged zone in adhesive layer in repaired structures by composites patches under thermo-mechanical loadings and a tensile stress σ = 150MP for a crack length a= 40 mm.

Since adhesive damage begins to be apparent at high temperatures, then we compare damaged adhesive surfaces only at temperature T=100°C for all shapes of corrosion.

Figure 7 shows the evolution of adhesive damaged area. It is noted that damaged zone is located around the crack for all the different patch types and all corrosion shapes. For this crack length, the damaged area is significant; indicating that the stresses at the crack front are sufficient to cause significant damage to the adhesive layer. This allows us to deduce that the adhesive damaged area can have an effect on the efficiency of the repair and durability of the bonded assemblies.

The damaged area develops around the crack and on the edge of adhesive layer at all figures. The damaged surfaces in the edge of adhesive layer are negligible comparing to the crack tip. Similarly, the damaged area includes a part of corrosion zone in the first model (with square shape corrosion), unlike the corroded plate in the second model (with circular shape corrosion), as it absorbs stress and appears only at the crack level and at the edges.

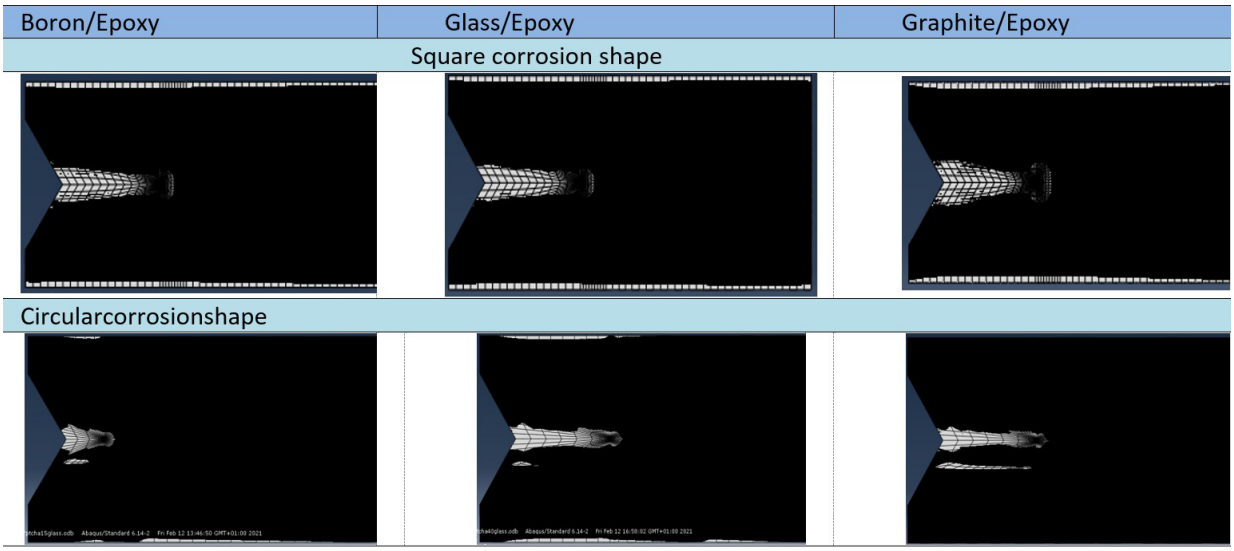

Figure 7 The damaged area of FM73 adhesive, for crack length a = 40mm.

2.1.5.2 Damaged area ratio D_R variations as function of crack length:

Figure 8 presents the variations of the D_R according to crack length for three types of composite at temperature T= 100°C for the two models of localized corrosion shapes (circular and square shape).

The variations of damaged area ratio D_R are increasing slightly from a point a = 5mm, but from the length of the crack a = 15 mm, the D_R increases considerably as a function of the increase of crack length. We note that the 03 types of patches did not reach the critical limit of the damaged area of the FM73 adhesive layer D_{RC} = 0.2474,in this case, all repaired models are resistant to failure. However, the plate with circular-corrosion gives the lowest DR values compared to the plate with square-corrosion, which makes it more efficient in reducing the risk of adhesive damage. As for the optimal type, we recorded after studying the DR values that Boron / Epoxy is the best type compared to other types.

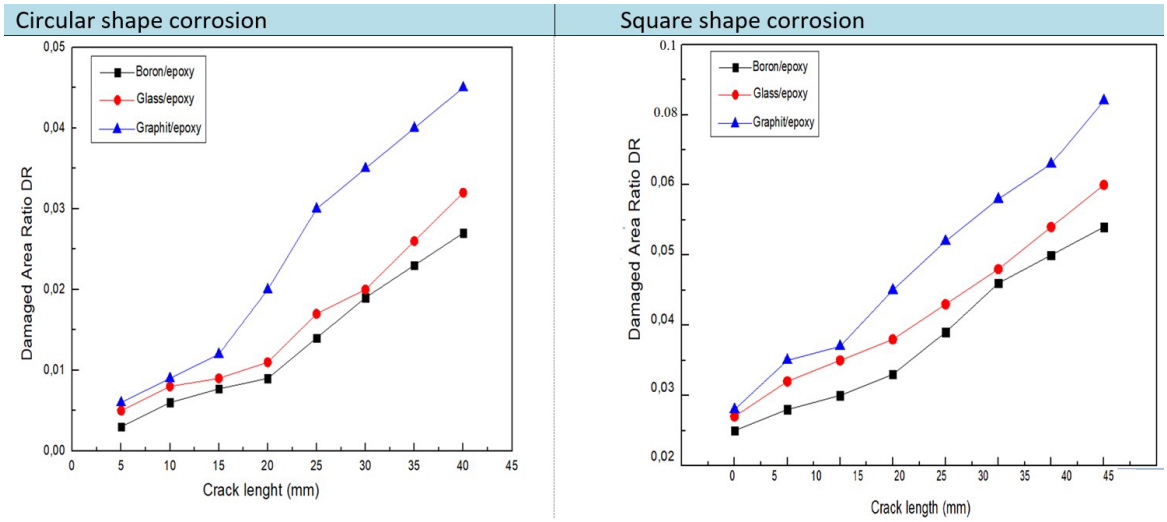

Figure 8 variations of $D_R$vs crack length for square and circular corrosion.

2.2 Experimental part

In this experimental study, we used AL 2024 aluminum alloy. To obtain the appropriate samples for the experiment, we accelerate the corrosion using water + salt basins, and then immerse these plates in this solution, and then we cut the 2024 alloy into several samples. These samples have a rectangular shape with dimensions (204x154x2) mm.

Aluminum is naturally covered with a layer of oxide, which often protects it from corrosion. In neutral aqueous solutions (4 < pH < 9), this oxide film is 50 Å thick and protects the metal (passivation), but chloride (Cl) ions have a very destabilizing effect on this oxide layer, then a rupture of the oxide layer occurs, which leads to corrosion. The following figures 9, 10, and 11 show the completed experiment stages to obtain corroded aluminum plates.

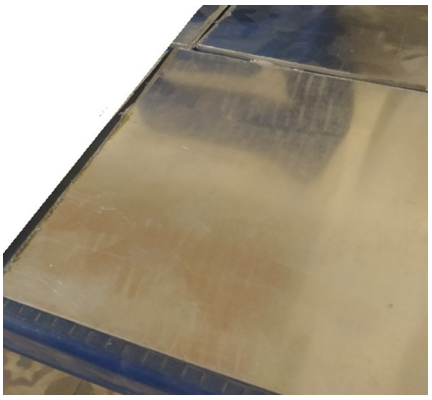

Figure 9 Before the process.

Figure 10 A week in process.

Figure 11 Three weeks after the operation.

The corroded plate repair procedures:

Through previous studies, we found that there are several solutions to repair the damaged structures with composite materials, which are determined above all according to the severity of the damage.

In this study, we focus only on the structural repair of corroded structures by adhesion of composite patches. This procedure is used to stop the corrosion growth in the aluminum plate, raise its efficiency, and restore its mechanical properties. In this experimental study, we focus only on investigation of the corrosion shape effects, we chose the boron / epoxy type patch for repair, since it has the optimal results in the analytical study compared to other types (glass/ epoxy and graphite / epoxy) with fiber orientation in the direction of the tensile strength (longitudinal direction).

The principle of these repairs is to remove the damaged area (the corrosion layer) and cover it with a composite patch. In the literature, several references (Salem et al.2019; Salem et al 2017; Benzineb et al. 2022)referred to the repair of composite materials by patches, which were classified into two categories: external and internal patches.

We have followed several steps to do this repair:

1- Preparing the corroded surface to be repaired: In order to stop the spread of corrosion in the structure, we begin by removing the laminated surface of all damaged corroded samples by rubbing the corrosion layer until reaching a healthy layer, by sanding and reactivating the surface with styrene (Figure 12).

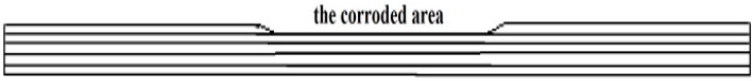

Figure 12 surface preparations before repair.

2- After the reactivation of the surface to be repaired, an attachment mat (300g mat) is placed on the two elements to be assembled, and then the lamination of the different layers of reinforcements is continued according to the sequence of the structure to be repair (Figure 13).

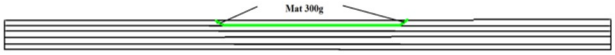

Figure 13 Illustration of the first stage of the repair.

3- In order to ensure the continuity of the part to be repaired, after the two components to be repaired are assembled, one is continued by sanding and reactivating the surface on which either external folds or glue are deposited.

Which the tensile properties were measured was according to the ASTM D3039-76 (ASTM 1990), where the ultimate strength is obtained. The ASTM D3039 tensile test is used to measure the force required to break the sample and how far the sample stretches or elongates to that breaking point. Tensile testing produces a stress–strain diagram which is used to determine the tensile properties.

2.2.1 Ultimate strength of the failure of different composites types for ambient temperature T=20°C

According to Figure 14, we can see that the longitudinal direction of circular corrosion shape has the best resistance to rupture since its maximum stress is the highest (300MPa) by a rate of 20% compared to the other shape of corrosion.

For the transverse direction, the resistance to failure was reduced to approximately a quarter of the longitudinal direction (Θ = 0°).The maximum pressure was at 83MPa for the plate with circular-corrosion. As for the other type of plate (with a square-shape), all the results recorded were lower than the net of the first plate.

For the longitudinal compressive and transverse compressive directions have the same behavior as the two other directions mentioned above. The compressive stress of plate with circular corrosion shape is one-third more efficient than the other shape of corrosion.

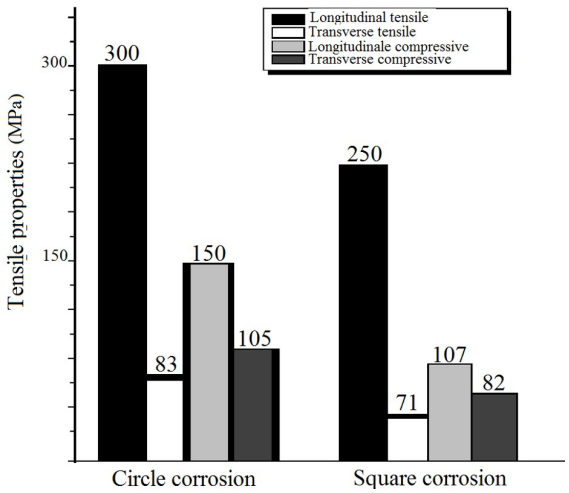

Figure 14 Tensile properties values as a function forseveral corrosion shape.

2.2.2 Study of ultimate strength as a function of temperature

This study is made to evaluate the loss of stiffness during the influence of varying temperatures on corroded aluminum plates, by accentuating the effect of corrosion shape on the safety of structures.

Figure 15 shows the variations in ultimate strength as a function of thermal variations for the corroded and cracked plate with different shapes of localized corrosion (circle or square shapes), repaired by composite patch (boron/epoxy), with longitudinal fiber orientations.

The failure resistance maintained its value near (240-300)MPa for a plate with circular corrosion and (170-250)MPa for a plate with square corrosion, until 60 °C of temperature for the fibers longitudinal , but after this value it begins to decline rapidly up to half (50%) at 80°C.

As for the comparison between the shapes of corrosion, we notice that the plate with square corrosion was more susceptible to damage than the plate with circular corrosion.

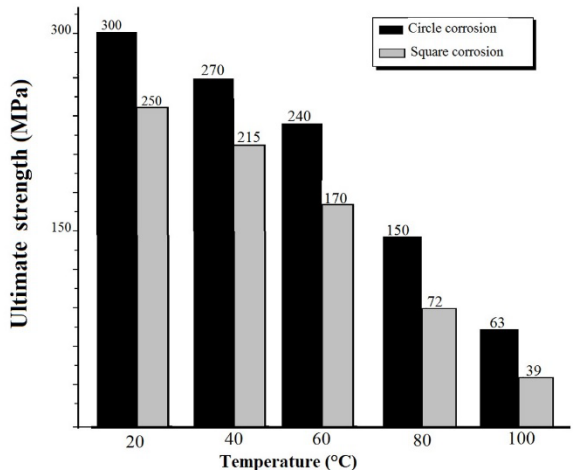

Figure 15 Ultimate strength values as a function of temperature for several corrosion shape.

3 CONCLUSIONS

Corrosion and crack effects are significant in metal a structure, which is why this study was conducted in two parts: an experimental part and a simulation part. The analytical part focused, using the finite element method, on evaluating the damaged area of the FM73 adhesive used in bonding structure, determining the stress intensity factor and then comparing the results to conclude which type of composite material and corrosion shape is better. In the experimental part, we compared the maximum ultimate strength of the damage of aluminum plates with a shape (circular and square) for corrosion repaired by boron/epoxy patch under thermal loading.

The obtained results show that the effects of corrosion geometry on the evolution of the constraints are significant, in addition to the effect of crack length under thermo-mechanical loads. As a result, we conclude the following observations:

- stress intensity factors (SIF) increase with increasing temperature
- Damaged area ratio (DR) variations increase with increasing temperature variations (ΔT).
- DR differences increase with increasing crack length.
- Boron/Epoxy is the optimal type of combination patch for this type of repair.
- The geometry of the circular localized corrosion has few effects compared to the square corrosion shape; the circular shape of corrosion is more absorbing stress and more efficient in resisting damage compared to the square corrosion shape**.**

Author's Contributions: Conceptualization, H Benzineb and M Berrahou; Methodology, H Benzineb; Investigation, , H Benzineb, M Berrahou and L Belkaddour; Writing - original draft, H Benzineb and M Berrahou; Writing - review & editing, H Benzineb; Funding acquisition, M Berrahou; Resources, L Belkaddour; Supervision, H Benzineb.

Editor: Marcílio Alves

References

ABAQUS/CAE Ver 6.9 (2007) User's Manual. Hibbitt, Karlsson & Sorensen, Inc.

Albedah,A.,Bouiadjra,B.B.,Mhamdia,R.,Benyahia, F., Es-Saheb, M. (2011). Comparison between double and single sided bonded composite repair with circular shape. Mater Des32:996–1000.

ASTM. (1990). ASTM standards and literature references for composite materials, Standard test method for tensile properties of fibers in composites D 3039-76, American Society for Testing and Materials, Philadelphia.

Benzineb, H., Berrahou, M., Serier, M. (2022). Analysis of the adhesive damage for different shapes and types patch's in corroded plates with an inclined crack. frattura ed integritàstrutturale16(60):331-345.

Benyahia,F.,Abdedah, A.,bouiadjra, B.B.(2014). Analysis of adhesive damage for different patch shapes in bonded composite repair of aircraft structures, Mater. Des 57:435–441.

Berrahou, M.,Bouiadjra, B.(2016). Analysis of the adhesive damage for different patch shapes in bonded composite repair of corroded aluminium plate, Structural Engineering and mechanics 59(1): 123–132.

Blond,J. B., Mouro, P. (1999). Crack propagation from a pre-existing flaw at a notch roat.I introduction and general form of Hu stress intensity factors at the initial crack tip. International journal of fracture. Springer Verlog 327:581–587.

Bouanani,M.F.,Benyahia,F.,Abdellah,A., Aid,A.,Bouiadjra,B. B.,Belhouari,M., Achour, T.(2013). Analysis of the adhesive failure in bonded composite repair of aircraft structures using modified damage zone theory, Mater. Des 50:433–439.

Bouchekara,N.M.H.,Abdellah,A.,Benyahia,F.,Khan Mohammed,S.M.A.,Bouiadjra B. B. (2021). Experimental and numerical analyses of the effects of overload of the fatigue life of aluminium alloy panels repaired with bonded composite patch. International journal and aeronautical space sciences 22:1075–1084.

Chang-Su, B., Young-Hwan, L., Jin-Ho,C., Jin-Hwe, K.(2008). Strength prediction of adhesive joints using the modified damage zone theory. Compos Struct 86:96–100.

Chegeni, B., Jayasuriya, S., Das, S. (2019). Effect of corrosion onthin-walled pipes under combined internal pressure and bending. Thin-walled structures 143:106–108.

Ely, M., Swiotowska, J., Seyeu, A., Zarma, S., Marcus, P. (2017). Pole of post-treatment in improved corrosion behaviour of trivalent chromium protection (TCP) coating deposited on aluminium alloy 2024 T3. Journal of the electronical society 164(6):276–284.

Hashimoto,T., Zhang,X., Zhou, X.,Skeldon,P.,Haigh,S.J., Thompson, G.E.(2016). Investigation of dealloying of S of Sphase (Al2CuMg) in AA 2024-T3 aluminium alloy using high resolution 2D and 3D electron imaging. Corrosion science 103:157–164.

Janssen, M. (2004). Fracture mechanics, Zuidema, J. (Jan), Wanhill, R. J. H. (2nd Ed.). London. Spon Press. p. 41. ISBN 0-203-59686-2. OCLC 57491375.

Karatzas,V. A.,Katsidis, E.,Tsouvalis, G.(2013). An experimental and numerical study of corroded steel plates repaired with composite patches. Analysis and design of marine structure- Guedes sores and romanoff (eds)13:405–412.

Liu,R.,Chu,T.,Li,L., Tateichi,K. (2019)A practical stress intensity factor formula for CFRP- repaired steel plates with a central crack. Journal of construction steel Research 162:105–755.

Nakano, H. Oue,S.Tagudi,S. abayashiS. and Horita,Z..(2012). Stress –corrosion cracking properties of aluminium-magnesium alloy processing equal-channel angular pressing. Intenational journal of corrosion.

Ramji,M.,Srilakhhmi,R., Bhanu Prakash, M.(2013). Towards optimisation of patch shape on the performance of bonded composite repaire using FEM. Compos. B Eng 45:710–720.

Rooke, D. P. and Cartwright, D. J. (1976). Compendium of stress intensity factors, HMSO Ministry of Defence. Procurement Executive.

Salem,M., Berrahou,M.,Mechab,B.,Bouiadjra, B.B.(2017). Effect of the angles of the cracks of corroded plate in bonded composite repair. frattura ed integritàstrutturale 46(1)113-123.

Salem, M., Serier, M., Berrahou M. (2019). Endommagement de l'adhésif d'une plaque corrodée et fissurée réparée sous chargement mécanique. 1ère conférences sur les energies renouvelables & les matériaux avancés erma'19 – relizane.834-840.

Sheppard, A., Kelly, D., Tong, L.(1998). A damage zone model for the failure analysis of adhesively bonded joints. Int Journal Adhes 18:385–400.

Shishesaz,M., Reza,A.(2013). The effect of viscoelasticity of adhesives on shear stress distribution in a double-lap joint using analytical method. Journal of Adhesion Science and Technology 27(20).

Soboyejo, W. O. (2003). Crack Driving Force and Concept of Similitude, J. Mechanical properties of engineered materials. Marcel Dekker. ISBN 0-8247-8900-8. OCLC 300921090.

Suresh, S. (2004). Fatigue of Materials, Cambridge University Press. ISBN 978-0-521-57046-6.

Umamahshwer Rao, A.C.,Vasu,V.,Govindaraju, M.,Sai Srindh, K. V. (2016). Stress corrosion cracking behaviour 7xxx Aluminium alloy. A literature reviex. Trans Nor ferreu. Met. Soc China 26:1447–1471.

Wang,Z., Chen, P., Li,H., Fang,B., Song,R., Zheng, Z.(2016). The intergranular corrosion susceptibility of 2024 Al alloy during re-aging after solution treating and cold-rolling. Corrosion science 114:156–168.

Wei,Y.,Wu,Z.,Wang,X.,Jiang,S.(2021). Mechanical behaviour of locally corroded circular steel tube under compression. Journal of Structures 33:776–791.

Xiaoyau,L.,Jiacheng,W.,Jiaojiao,X., Zhiqiang,Y. (2019). Bonded Repair optimisation of cracked Aluminium Alloy plate by microwave cured carbon-aramid fiber/epoxy.Materials 12(10):1655.